Bispecific GPC3/PD-1 CAR-T cells for the treatment of HCC

DEZHI LI[1*], JIE QIN[2*], TAO ZHOU[1], YAQIN LI[3], XIANYI CHENG[1], ZAIZHONG CHEN[1], JUNHUI CHEN[1] and WEI V. ZHENG[1]

[1]Intervention and Cell Therapy Center; [2]Department of Scientific and Research; [3]Department of Infectious Disease, Peking University Shenzhen Hospital, Shenzhen, Guangdong 518036, P.R. China

Received April 28, 2022; Accepted September 6, 2022

DOI: 10.3892/ijo.2023.5501

Abstract. Constantly stimulated by the tumor microenvironment (TME), programmed death 1 (PD-1) is elevated, and it interacts with PD ligand 1 (PD-L1), rendering chimeric antigen receptor (CAR)-T cells dysfunctional. Hence, CAR-T cells immune to PD-1-induced immunosuppression were constructed to improve the function of CAR-T cells in hepatocellular carcinoma (HCC). Double-target CAR-T cells, targeting glypican-3 (GPC3) [a tumour-associated antigen (TAA)] and hindering PD-1-PD-L1 binding, were established. The expression of GPC3, PD-L1, and inhibitory receptors was measured using flow cytometry. The cytotoxicity, cytokine release, and differentiation level of CAR-T cells were determined using lactate dehydrogenase release assay, enzyme-linked immunosorbent assay, and flow cytometry, respectively. HCC cells were targeted and eliminated by double-target CAR-T cells. These double-target CAR-T cells limit PD-1-PD-L1 binding and sustain cytotoxicity to PD-L1$^+$ HCC cells. The relatively low IR expression and differentiation level in double-target CAR-T cells in tumour tissues induced tumour-suppression and extended survival in PD-L1$^+$ HCC TX models, as opposed to their single-target counterparts. The results of the present study suggested that the newly constructed double-target CAR-T cells exhibit stronger tumour-suppressing effects in HCC than their single-target counterparts, which are common, suggesting the potential of strengthening CAR-T cell activity in HCC treatment.

Correspondence to: Dr Junhui Chen or Dr Wei V. Zheng, Intervention and Cell Therapy Center, Peking University Shenzhen Hospital, 1120 Lianhua Road, Shenzhen, Guangdong 518036, P.R. China
E-mail: chenjhpush@126.com
E-mail: zhengw2020@yeah.net

*Contributed equally

Key words: glypican-3, programmed death 1, chimeric antigen receptor, hepatocellular carcinoma, cancer immunotherapy

Introduction

According to Global Cancer Incidence, Mortality and Prevalence (GLOBOCAN) 2020, hepatocellular carcinoma (HCC) is the third highest cause of cancer-related mortality globally, and a devastating disease with a high prevalence and unsatisfactory prognosis. There are ~906,000 new cases and 830,000 deaths of primary liver cancer in 2020, of which HCC accounted for 75-85% of cases (1,2). The risk factors of HCC are chronic hepatitis, hepatitis B virus (HBV)/HCV infection-triggered cirrhosis, alcoholic cirrhosis, dietary aflatoxin exposure, non-alcoholic steatohepatitis, α-1-antitrypsin deficiency and hemochromatosis (3). This disease may be cured through liver transplantation or resection, but these surgical schemes are not suitable for the majority of patients late in the disease course (4). The 5-year survival rates for HCC in China are <12.5%, thus effective treatment schemes for HCC require further investigation (5).

Glypican-3 (GPC3), a member of the heparan sulfate proteoglycan family, is a cell-surface glycophosphatidylinositol-anchored protein (6,7). GPC3 is highly expressed in at least 70% of HCC patients but not in normal adult tissues (8-10). GPC3 has been suggested to be an important diagnostic biomarker and immunotherapeutic target for HCC (11-13). Preclinical studies performed by Shi *et al* (14) confirmed the potential of GPC3-chimeric antigen receptor (CAR)-T cell therapy for HCC.

CAR comprises an extracellular antigen recognition domain (ARD), an intra-cellular signaling domain (i.e. CD3ζ) with or without 1 or 2 costimulatory molecules, and a transmembrane domain (15). CAR-T cells can distinguish the exact tumour-associated antigens (TAAs) in a manner independent of the major histocompatibility complex (16-18). Nowadays, although the curative effect of CAR-T cell therapy has been proven to treat hematological malignancies (19), it remains unsatisfactory in treating solid tumours (20,21). In contrast to blood tumours, solid tumours have an immunosuppressive tumor microenvironment (TME), which induces the expression of PD-1 on CAR-T cells. PD-1/PD-L1 axis is a well-known immune checkpoint inhibitor pathway. The combination of PD-L1 and PD-1 generates an inhibitory signal that prevents T cell activation, enabling tumour cells to escape from the monitoring of the immune system (22,23). Hence, CAR-T cells should be somewhat modified to avoid this inhibitory signal of the PD-1/PD-L1 pathway in HCC.

A double-target CAR with an extracellular ARD containing anti-PD-1 single-chain fragment variable (scFv) and anti-GPC3 scFv was established to help CAR-T cells persistently resistant to PD-1 inhibitory signals. It was hypothesized that the double-target CAR is capable of targeting tumour cells via anti-GPC3 scFv and blocking PD-1 which was expressed on para-tumour CAR-T cells via anti-PD-1 scFv. It appears that the newly-established double-target CAR-T cells were more effective in reducing tumor burden and prolonging the survival of tumor xenograft models than traditional single-target CAR-T cells, representing an effective strategy for applying CAR-T cell therapy to solid tumours.

Materials and methods

Cells and cell culture. HCCLM3 and HuH7 cells were obtained from China Center for Type Culture Collection, and SNU423, SNU182 and 293T cells were obtained from the American Type Culture Collection. Primary T cells from humans were cultured in a 37˚C cell incubator (5% CO_2) containing RPMI-1640 medium (MilliporeSigma) containing recombinant human IL-2 (30 IU/ml; cat. no. Z00368-1; GenScript), 10% fetal bovine serum inactivated by heat and 1% penicillin-streptomycin (Cytiva).

Preparation and transduction of vectors and lentiviruses. In the present study, the established CAR encompassed an extracellular ARD, a CD8 hinge, a CD28 transmembrane domain, a CD28 combined with or without 4-1BB domain, and a CD3ζ-derived signal transduction domain. A pKC lentiviral vector (BioVector NTCC, Inc.) was sub-cloned with discrepant CAR sequences in the frame.

Then this vector, together with packaging plasmid r-8.91, enveloping protein plasmid vesicular stomatitis virus G (1 μg: 900 ng: 100 ng), was used for 293T cell transfection using a PEIpro® transfection reagent (Getong Technology Co., Ltd.). The virus-containing supernatants were collected 48 and 72 h later, and an Amicon Ultra-15 centrifugal filter from MilliporeSigma was used to enrich the virus. In addition, a human T cell enrichment cocktail (cat. no. 15061; RosetteSep™; Stemcell Technologies, Inc.) was used for primary T cell isolation from the peripheral blood of tumor-free volunteers. The volunteers were health examiners in our hospital (samples were collected between March-April 2021), including 2 males and 2 females, aged 32-50 years, with an average of (40±7.8) years. The use of human peripheral blood was approved (approval no. 2021-081) by the Ethics Committee of Peking University Shenzhen Hospital (Shenzhen, China) and all donors provided informed written consent. Next, monoclonal antibodies (mAbs; 5 μg/ml) against pre-enveloped CD3 (cat. no. 05121-25-500) and dissolvable CD28 (cat. no. 10311-25-500; both from PeproTech, Inc.) were used to activate the obtained cells for 48 h prior to lentiviral infection. Next, T cell treatment with polybrene (8 μg/ml) was conducted for 4 h, followed by transduction with lentivirus enriched on the plate enveloped by NovoNectin (cat. no. CH38; Novoprotein Scientific, Inc.) plates for 8 h at 37˚C (multiplicity of infection: 3). After 48 h, CAR expression was examined. Empty lentivirus was used as control.

Reverse transcription-quantitative (RT-q) PCR. Total RNA was isolated using Qiagen RNeasy Mini kit (Qiagen, Inc.), according to the manufacturer's instructions and cDNA synthesis was completed using the High Capacity cDNA Reverse Transcription kit (Applied Biosystems; Thermo Fisher Scientific, Inc.) according to the manufacturer's protocol. qPCR was performed under the following thermocycling conditions: 10 min at 95˚C, 40 cycles of 15 sec at 95˚C and 1 min at 60˚C. qPCR was performed using 2X SYBR-Green PCR Master mix (Beijing Solarbio Science & Technology Co., Ltd.) and 200 nM forward and reverse primers for Bcl-2 and caspase-3. GAPDH was used as a reference gene. The sequences of the primers used were as follows: Bcl-2 forward, 5'-AAAAATACAACATCACAG AGGAAGT-3' and reverse, 5'-GTTTCCCCCTTGGCATGA GA-3'; caspase-3 forward, 5'-TGCTATTGTGAGGCGGTT GT-3' and reverse, 5'-TTAACGAAAACCAGAGCGCC-3'; and GAPDH, forward, 5'-CTGGGCTACACTGAGCACC-3' and reverse, 5'-AAGTGGTCGTTGAGGGCAATG-3'. Each assay was run on an Applied Biosystems 7300 Real-Time PCR System (Applied Biosystems; Thermo Fisher Scientific, Inc.) in triplicate, and the fold-changes of gene expression were derived using the comparative $2^{-\Delta\Delta Cq}$ method, as previously described (24).

Flow cytometry (FC). mAbs against FITC-PD1 (1:20; cat. no. 329903), PE-PD-L1 (1:20, cat. no. 329705), FITC-CD69 (1:20; cat. no. 310903), FITC-CD3 (1:20; cat. no. 317305), FITC-Annexin V (1:20; cat. no. 640905), FITC-CD62L (1:20; cat. no. 304803), FITC-CD45RA (1:20; cat. no. 304105), FITC-CD45 (1:20; cat. no. 304006), APC-Granzyme B (1:20; GrB; cat. no. 372203), FITC-perforin (1:20; cat. no. 353309; all from BioLegend, Inc.), and FITC-GPC3 (1:20; cat. no. 100393-R024; Sino Biological) were used. Following rinsing twice with PBS, the cells were dyed and underwent 20-min mAb incubation (5 μl per million cells in 100 μl staining volume) at 4˚C protected from light, and they were assessed after they were immobilized in PBS.

To detect CAR expression on CAR-T cells, the cells were stained with biotinylated protein L (cat. no. M00097; GenScript) and then stained with streptavidin-PE at 37˚C for 10 min (cat. no. 405203; BioLegend, Inc.). Flow cytometry data were acquired on a Gallios flow cytometer (Beckman Coulter, Inc.) and analyzed using the FlowJo software (Tree Star, Inc.). The level of expression of CAR on each type of CAR-T cell was adjusted to the same level by un-transduced T cells before use.

$PD\text{-}1^+$ CAR-T cells were obtained by stimulating CAR-T cells with pre-coated anti-CD3 and soluble anti-CD28 antibodies for one week to induce PD-1 expression. Finally, the obtained cells were dyed at 4˚C for 15 min. using FITC-PD-1 mAb and distinguished from their $PD\text{-}1^-$ counterparts using FITC fluorescence.

Cytokine investigation. ELISA (cat. nos. KGEHC102g, KGEHC003 and KGEHC154; Nanjing KeyGen Biotech Co., Ltd.; and cat. no. K4279-100; AmyJet Scientific, Inc.) was performed after gathering the supernatants/sera from mice, in order to clarify whether granzyme B (GrB), interferons (IFN)-γ, perforin and IL-2 exist.

In vitro CAR-T cell proliferation assays. HuH7 cells were stimulated with IFN-γ (40 μg/ml) for 8 h to induce the expression of PD-L1 and then inactivated with mitomycin C (100 μg/ml; cat. no. MB1164; Dalian Meilun Biology Technology Co., Ltd.) at 37˚C for 2 h. Every 4 days, the cells were collected following inactivation to provoke each group of CAR-T cells (10^5/well), and the CAR-T cells were counted. Next, uninfected T cells (control) were cultured using 30 IU/ml recombinant IL-2. FC was ultimately used to distinguish the CAR-T cell phenotype.

Cell toxicity and death rate. A lactate dehydrogenase (LDH) assay was used to measure CAR-T cell toxicity using the corresponding kit (cat. no. C0016; Beyotime Institute of Biotechnology). CAR-T cells ($1x10^5$) were co-cultured with the target cells at various effector to target (E:T) ratios (4:1, 8:1, 16:1 and 32:1). The working concentration of the anti-PD-1 mAb (cat. no. 201905014; TopAlliance Biosciences) combined with GPC3-CAR-PD-1^+ T cell was 10 μg/ml. The overall volume of the cultured system was 100 μl and was incubated for 12 h at 37˚C in 96-well plates. Cell toxicity was calculated as follows: Cell toxicity (%)=(mixture cell experiment - effector cell spontaneous-target cell spontaneous-medium control)/(target cell maximum-target cell spontaneous-medium control) x100%.

Subsequently, the corresponding cells were cultured in media comprising GrB (cat. no. ENZ-855; ProSpec-Tany TechnoGene, Ltd.) with/without perforin (cat. no. APB317Mu01; Cloud-Clone Corp.) for 12 h. Next, an LDH assay kit was used to calculate the cell death rate as follows: Cell death rate (%)=(cell experiment-cell spontaneous-medium control)/(cell maximum-cell spontaneous-medium control) x100%.

TX assays. All experimental procedures in the present study were approved (approval no. 2021-081) by the Ethics Committee of Peking University Shenzhen Hospital (Shenzhen, China). A total of 24 female NOD/SCID mice (4-6 weeks old, 6 in each group) were housed at the Laboratory Animal Center of Peking University Shenzhen Hospital. Mice were housed in a sterile room under a 12-h light/dark cycle at ~23˚C and 50% humidity, with *ad libitum* access to food and water. A total of $5x10^6$ HuH7 cells in 100 μl PBS were subcutaneously injected into the right flank of mice to establish the TX model. Once the average tumor size reached 100-200 mm^3, the mice were randomly assigned to different groups. A total of $1x10^6$ CAR-T cells in 100 μl PBS were injected intratumorally into each mouse and the tumors were measured weekly post-injection. In the CAR-T cells combined with anti-PD-1 group, each mouse was intraperitoneally injected with 150 mg anti-PD-1 mAb once a week (a total of 5 times). The tumor volume was calculated according to the formula $V=(\text{length} \times \text{width}^2)/2$. The health and behaviour condition of mice was monitored daily. On day 42 or when a humane endpoint had been reached (e.g., >25% body weight loss, signs of illness or distress including ruffled fur, difficulty with diet, or abnormal posture), mice were euthanized and dissected for tumor tissue analysis. Euthanasia was performed using an intravascular administration of an overdose of sodium pentobarbital (200 mg/kg) followed by cervical dislocation. Euthanasia was confirmed by the loss of vital signs, such as respiration and heartbeat cessation.

Immunohistochemistry (IHC). Tumor tissue was fixed with 4% formaldehyde at 37˚C for 24 h, embedded in paraffin and sectioned into a thickness of 2-μm. Following dewaxing with xylene, hydration in alcohol with different concentrations, tissue incubation in hydrogen peroxide (3%) was performed to quench endogenous peroxidase and sodium citrate buffer (0.01 M, pH 6.0) was used to retrieve antigens at 95˚C. Using 1% bovine serum albumin (Azer Scientific, Inc.), the slide blocking lasted for 30 min at room temperature. The sections were sequentially incubated with primary antibodies at 4˚C overnight, including anti-Ki-67 (1:5,000; cat. no. 27309-1-AP;), anti-VEGF-A (cat. no. 19003-1-AP; 1:500; both from ProteinTech Group, Inc.), anti-MMP-9 (cat. no. 13667; 1:500; Cell Signaling Technology, Inc.). On the next day, slides were incubated with HRP-conjugated secondary antibodies (1:1,000; cat. no. 7074S; Cell Signaling Technology, Inc.) for 40 min at room temperature. After scanning IHC sections, images were captured using CaseViewer 2.2 (3DHISTECH Kft).

Western blot analysis. The cell lysate was obtained using 2% SDS and then centrifuged (4˚C, 12,000 x g, 15 min) to obtain the supernatants. The protein concentration was detected using a BCA protein assay kit (cat. no. 23225; Thermo Fisher Scientific, Inc.). A total of 20 μg protein was separated using a 3% SDS-PAGE and transferred to a PVDF membrane. The transferred PVDF membrane was blocked using 5% skimmed milk for 1 h at 25˚C and washed with Tris-buffered saline with Tween 20 (TBS-T) (1% Tween 20) (cat. no. 170-6435; Bio-Rad Laboratories, Inc.), then incubated with primary antibodies for 10 h at 4˚C and incubated with the secondary antibodies at room temperature for 1 h. Finally, the membrane was visualized using the ImageQuant™ LAS 4000 system (Cytiva). Anti-GPC3 (1:1,000; cat. no. ab124829), anti-PD-L1 (1:1,000; cat. no. ab243877), Goat Anti-Rabbit IgG H&L (HRP) (1:5,000; cat. no. ab6721) and rabbit anti-human GAPDH (1:2,500; cat. no. ab9485; all from Abcam) were used. The protein bands were analyzed using ImageJ software (version 1.48; National Institutes of Health).

Data assessment. All data analyses were performed using GraphPad Prism version 7.0 (GraphPad Software, Inc.). One-way analysis of variance (ANOVA) followed by Bonferroni test or unpaired t-tests were used to compare different groups. The Kaplan-Meier method and log-rank test were used to assess the survival curves of the mice. $P<0.05$ was considered to indicate a statistically significant difference.

Results

Establishment and expression of double-target CAR molecules. Double-target CAR, known as GPC3/PD-1-CAR, which could recognize PD-1 in T cells and GPC3 in tumour cells, was established. Next, anti-GPC3 scFv was connected to anti-PD-1 scFv using a GGGGS linker, which is used to bind the antigen outside the cell. Through a CD8 hinge and a CD28 transmembrane domain, the extracellular antigen binding domain (ABD) is connected to the intra-cellular domain. The intra-cellular domain consisted of the CD3ζ-chain, CD28 and 4-1BB (2 costimulatory domains). To investigate the effects of the sequential order of anti-PD-1 scFv and

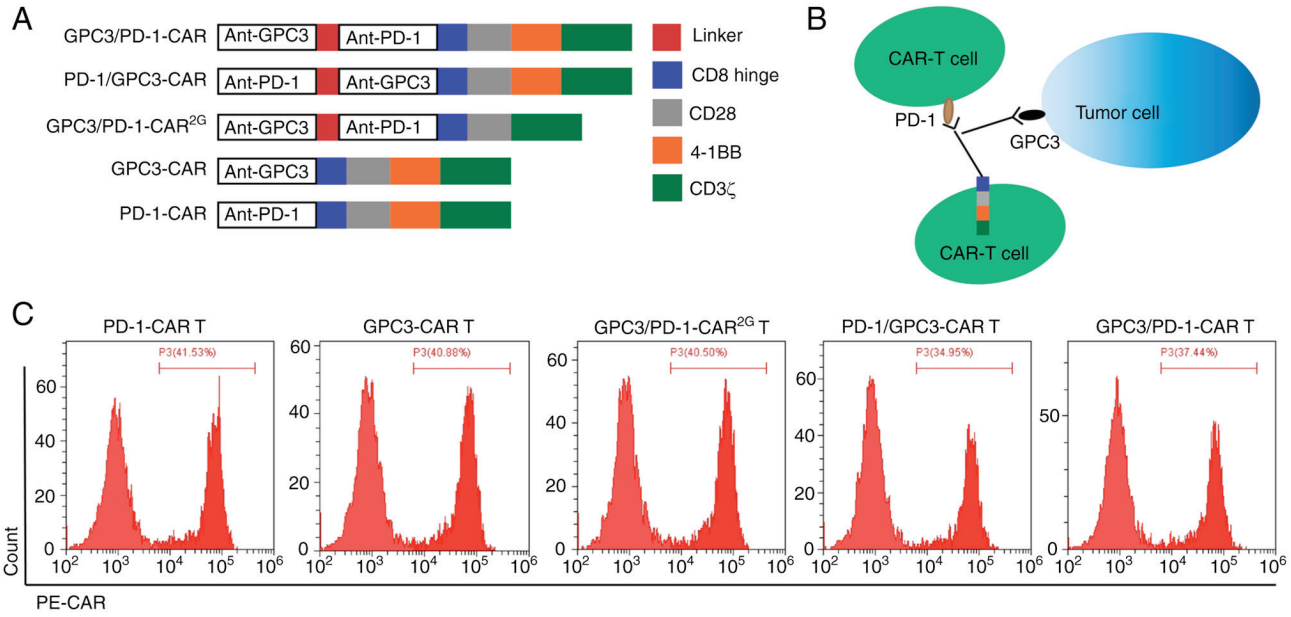

Figure 1. Establishment and expression of the double-target CAR molecules. (A and B) Diagram of a lentiviral vector encoding CARs. (C) FC results for the measurement of CAR expression in T cells. CAR, chimeric antigen receptor; FC, flow cytometry.

anti-GPC3 scFv on the function of dual-function CAR, the sequential order of the two scFvs in GPC3/PD-1-CAR was changed, constructed as PD-1/GPC3-CAR. Anti-GPC3 scFv and anti-PD-1 scFv were extracellular ABDs of GPC3-CAR and PD-1/CAR (two single-target CARs), and their other structures were the same as those of double-target CARs. The aforementioned CAR structures are all three-generation CARs containing two co-stimulation domains of CD28 and 4-1BB. GPC3/PD-1-CAR^{2G}, a 2G double-target CAR, was also established, which comprised only CD28, for the purpose of comparing the functions of 2G and 3G CARs. Except where noted, the CARs in the present study were of the third generation (CAR^{3G}). Fig. 1A is a diagram of the role of established CARs. Fig. 1B is a diagram of the role of double-target CAR-T cells. FC was used to measure differences in the expression of CARs in T cells. As revealed in Fig. 1C, the FC results exhibited a positive CAR expression on T cells (positive rate 34.95-41.53%).

The established CARs have specific reactions to target antigens. Recombinant PD-1 and GPC3 proteins were used to provoke CAR-T cells, in order to clarify the function of the established CARs on certain reactions to target antigens. Provoked by target antigens, the expression level of CD69 (an earliest marker elevated after T cell activation) in CAR-T cells was examined. Following stimulation by GPC3 and PD-1, a pronounced elevation of CD69 was discovered in GPC3/PD-1-CAR (positive rate 75.06%) and PD-1/GPC3-CAR (positive rate 72.99%) T cells, and a modest elevation was observed in PD-1-CAR (positive rate 47.45%) and GPC3-CAR (positive rate 48.04%) T cells (Fig. 2A). This provoking also resulted in a higher IFN-γ and IL-2 secretion in CAR-T cells compared with control cells (Fig. 2B and C). Beyond that, GPC3-CAR-T and PD-1-CAR-T cells displayed a lower CD69 expression level and lower cytokine secretion compared with double-target CAR-T cells (Fig. 2A-C).

The aforementioned results showed the targeted control of the established CARs on active signals, and the provoking effect of the 2 targets on cells, i.e., under the provoking of the 2 targets, dual-function CAR-T cells mediated a stronger active signal.

Double-target CAR-T cells display targeted toxicity to HCC cells. Western blotting was performed to measure the expression of GPC3 and PD-L1 in SNU182, HCCLM3, HuH7 and SNU423 cells. It appeared that the two targets (GPC3 and PD-L1) were expressed in all four HCC cell lines (Fig. S1A).

As specified in the 'Cell toxicity and death rate' section, the LDH assay revealed that with un-transduced T cells as controls, GPC3/PD-1-CAR-T cells successfully eliminated SNU182, HCCLM3, HuH7 and SNU423 cells at discrepant E:T ratios (Fig. 3A). Next, it was explored whether the expression level of GPC3 impacted the function of GPC3/PD-1-CAR-T cells. It was revealed that GPC3 expression was knocked down in HuH7 cells via GPC3 shRNA transfection (Fig. S1B); these cells were called HuH7(sh-GPC3). Next, HuH7(sh-GPC3) and HuH7 cells were cultured with GPC3/PD-1-CAR-T cells at different E:T ratios, and cell toxicity was determined using LDH assay. GPC3/PD-1-CAR-T cells were more efficient in eliminating HuH7 than HuH7(sh-GPC3) cells (Fig. 3B).

Furthermore, the differences among the activity of the four types of CAR-T cells co-cultured with HuH7 cells showed that toxicity and cytokine secretion were analogous for the two 3G double-target CAR-T cells, but they were superior to those of GPC3-CAR-T and GPC3/PD-1-CAR^{2G}-T cells (Fig. 3C and D).

These results indicated that T cells of dual-functional CAR and GPC3-CAR can mediate robust cytotoxicity to tumor cells in a target-dependent manner and the killing efficiency of these cells is positively correlated with GPC3 expression. GPC3/PD-1-CAR were selected for later research in light of the analogous activity of the two classes of double-target CARs.

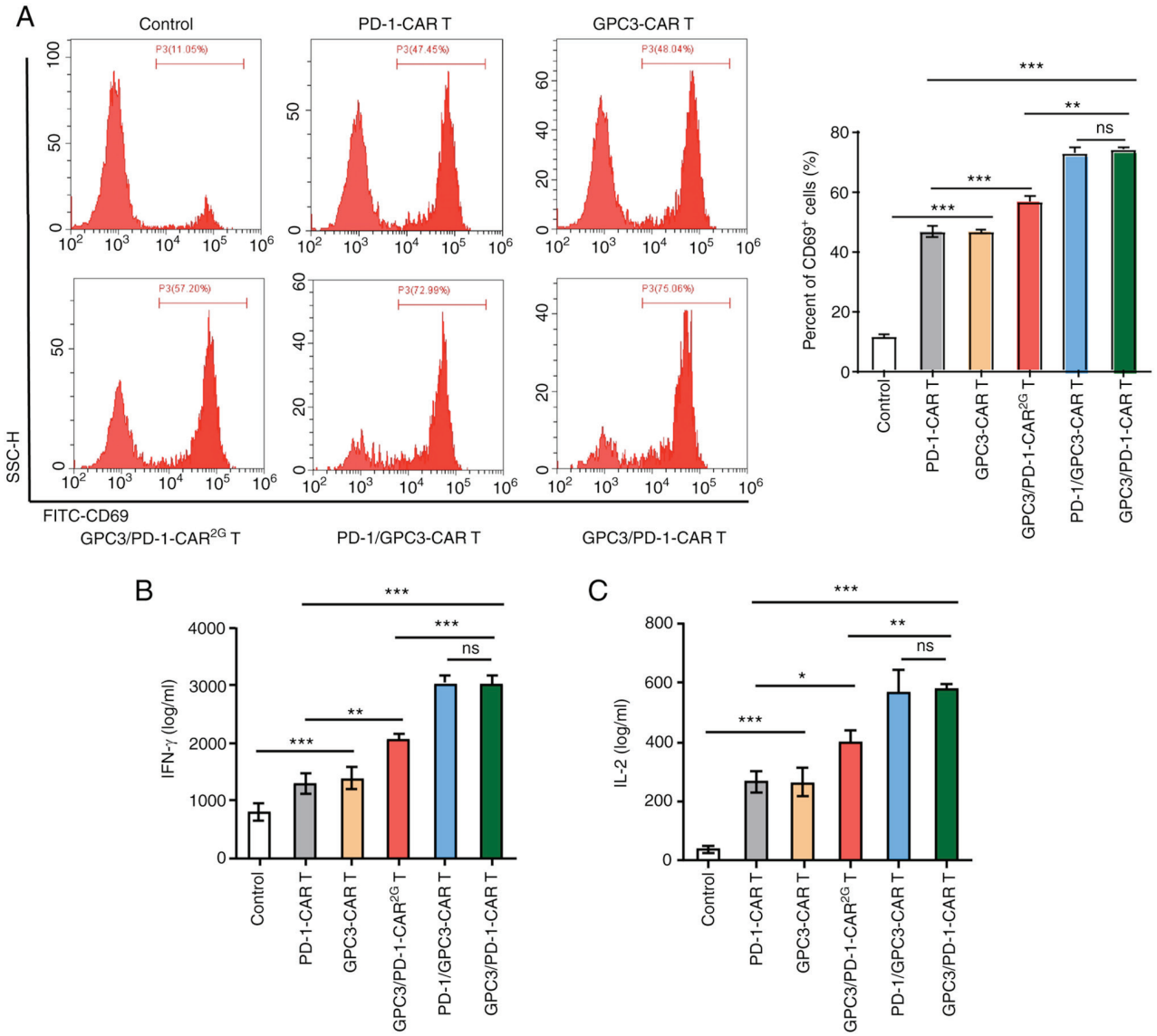

Figure 2. Established CARs have specific reactions to target antigens. (A) Characteristic FC (left) and histograms (right) of CD69 expression levels of different CAR-T cells following 12 h of provoking by target antigens (recombinant human GPC3 and PD-1 proteins). (B and C) Concentrations of IL-2 and IFN-γ released by the different CAR-T cells secreted upon encountering target antigens for 24 h, as examined by ELISA. Data are presented as the mean ± SD. *P<0.05, **P<0.01 and ***P<0.001. ns, not significant; CAR, chimeric antigen receptor; FC, flow cytometry; GPC3, glypican-3; PD-1, programmed death 1.

To determine the presence of targeted toxicity of double-target CAR-T cells to T cells expressing PD-1, T cells underwent 1 week of incubation with pre-coated anti-CD3 and soluble anti-CD28 antibodies to obtain PD-1^{+} T cells. Next, PD-1^{+} T cells, unprovoked T cells (T cells), and HuH7 cells were co-cultured with double-target CAR-T cells, respectively, at discrepant E:T ratios. As shown by the results of the LDH assay, double-target CAR-T cells exhibited no strong killing activity against T cells with different PD-1 expression levels (Fig. 3E).

The cause of insignificant toxicity of double-target CAR-T cells to T cells expressing PD-1 was examined by culturing HuH7 cells in a cascade of media containing different concentrations of GrB and perforin. When the cell death rate reached ~60%, GrB and perforin concentrations reached 0.5 and 0.25 μg/ml, respectively (Fig. 3F). Next, medium containing 0.5 μg/ml GrB and 0.25 μg/ml perforin was utilized to compare the death rates of HuH7, PD-1^{+} T and T cells, with a normal medium used as the control. In the GrB- and perforin-containing culture medium, PD-1^{+} T cell and T cell death rates exhibited slight upward trends, which were significantly lower than that of HuH7 cells (Fig. 3G). A higher tolerance of T cells to GrB and perforin were observed, and both indices are markers for the killing of target cells by CAR-T cells. This deciphered the cause of insignificant toxicity of double-target CAR-T cells to PD-1^{+} T cells.

Double-target CAR-PD-1+ T cells have enhanced toxicity to tumour cells highly expressing PD-L1. CAR-T cells were stimulated with precoated anti-CD3 and soluble anti-CD28 antibodies for 1 week to construct CAR-PD-1^{+}-T cells, and then FACS was adopted to get CAR-PD-1^{+}-T and CAR-PD-1^{-}-T cells. HuH7 cells were also provoked using IFN-γ to induce PD-L1 expression, and PD-L1^{+}-HuH7 cells were subsequently used to determine cell toxicity.

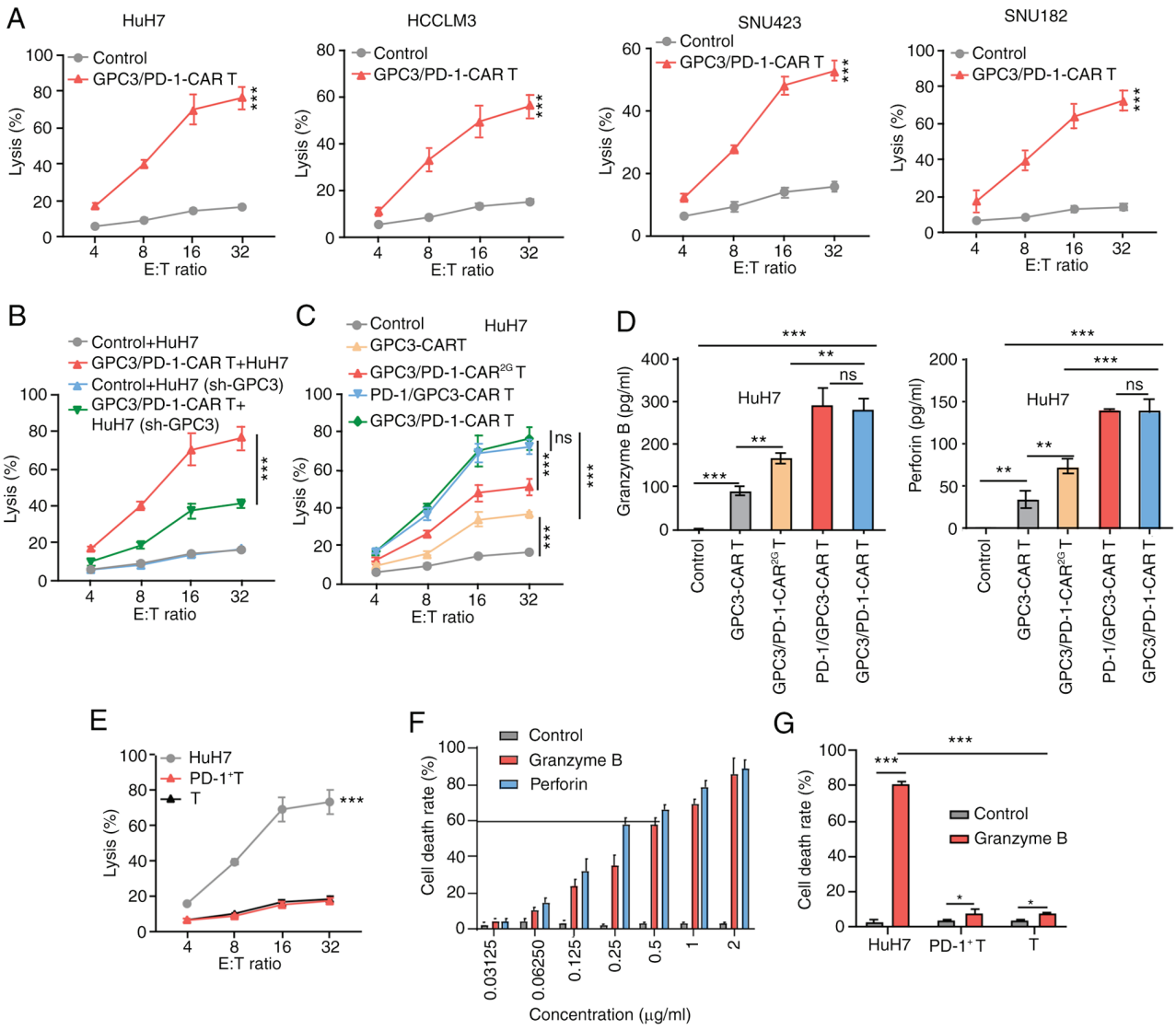

Figure 3. Double-target CAR-T cells show cytolytic potency to target HCC cells. (A) Cytotoxicity of GPC3/PD-1-CAR-T cells to the four indicated HCC cell lines at various E:T ratios evaluated by an LDH cytotoxicity assay. (B) Comparison of the toxicity of GPC3/PD-1-CAR-T cells to HuH7 cells with different GPC3 levels at E:T ratios of 4:1, 8:1, 16:1 and 32:1. Un-transduced T cells served as control. (C) Comparison of the toxicity of various CAR-T cells against HuH7 at different E:T ratios. Un-transduced T cells served as control. (D) Levels of GrB and perforin measured using ELISA after co-culturing different CAR-T cells with HuH7 at an E:T ratio of 1:1 for 24 h. (E) Comparison between the cytotoxicity of GPC3/PD-1-CAR-T cells and that of HuH7, PD-1+ T and T cells at various E:T ratios, as assessed by an LDH assay. (F) The death rate of HuH7 cells under a series of concentrations of GrB and perforin for 12 h. (G) The death rates of HuH7, PD-1+ T and T cells after co-culturing in the indicated culture medium for 12 h. Data are presented as the mean ± SD. *P<0.05, **P<0.01 and ***P<0.001. ns, not significant; CAR, chimeric antigen receptor; HCC, hepatocellular carcinoma; GPC3, glypican-3; PD-1, programmed death 1; E:T, effector-to-target; LDH, lactate dehydrogenase; GrB, granzyme B.

The dual-function and single-target CAR-PD-1^{+} -T cells were co-cultured with PD-L1^{+} -HuH7 cells at 1:1 ratio for 3 days, and the residual targeted cells were examined using FC. The marker was GPC3 for HuH7 cells and CD3 for CAR-T cells. The PD-L1^{+} -HuH7 cells continued to grow in co-culture with GPC3-CAR-PD-1^{+}-T cells, suggesting that the activation of the CAR-T cells may be dampened by the PD-1/PD-L1 pathway (Fig. 4A). Conversely, double-target CAR-PD-1^{+}-T cells were capable of successfully limiting the target tumours despite PD-1 expression.

Through the combination of an mAb against human PD-1 with GPC3-CAR-PD-1^{+}-T cells, it was sought to interrupt the PD-1/PD-L1 pathway in eliminating PD-L1^{+} -HuH7 cells and this combination strategy was compared with double-target CAR-PD-1^{+}-T cells. It appeared that double-target CAR-PD-1^{+}-T cells had stronger cytolytic effects at E:T ratios of 4:1 and 8:1 to PD-L1^{+}-HuH7 cells, as compared with the combination strategy (Fig. 4B). In addition, double-target CAR-PD-1^{+}-T cells secreted more cytokines at an E:T ratio of 4:1 compared with the secretion observed following the combination regimen (Fig. 4C).

Double-target CAR-T cells exhibit a decreased inhibitory receptor (IR) expression, increased proliferation and subdue terminal differentiation in long-time antigen stimulation. Inactivated tumour cells were used to provoke GPC3-CAR-T and GPC3/PD-1-CAR-T cells every 4 days for 24 days under no other stimuli, and the expression, differentiation and proliferation of IRs was measured at 8, 16 and 24 days to determine the effect of PD-1 blocking

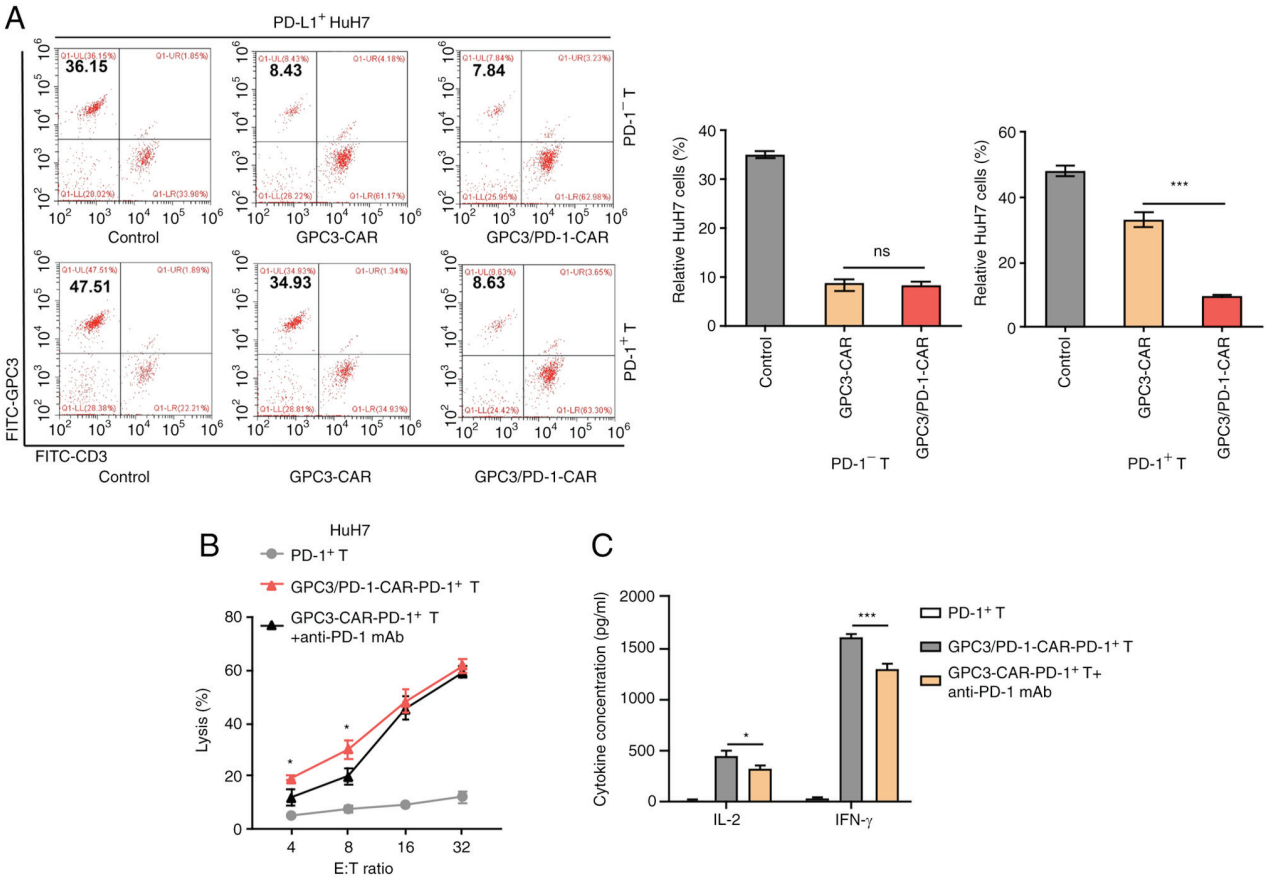

Figure 4. Double-target CAR-PD-1+ T cells exhibit high toxicity to tumour cells that highly express PD-L1. (A) Characteristic FC diagrams of the percentages of residual PD-L1$^+$-HuH7 cells after a 3-day coculture with CAR-PD-1$^+$-T or CAR-PD-1$^-$T cells at an E:T ratio of 1:1 (left). GPC3 is a marker for HuH7 cells and CD3 for CAR-T cells. Un-transduced PD-1$^-$-T or PD-1$^+$-T cells were used as controls. Measurement of ratios of residual tumour cells in each paired group (right). (B) Comparison of the cytotoxicity of GPC3/PD-1-CAR-PD-1$^+$-T and GPC3-CAR-PD-1$^+$-T cells combined with anti-PD-1 mAb to PD-L1$^+$-HuH7 at different E:T ratios. (C) Concentrations of IL-2 and IFN-γ after co-culturing GPC3/PD-1-CAR-PD-1$^+$-T cells and GPC3-CAR-PD-1$^+$-T cells + anti-PD-1 mAb with PD-L1$^+$-HuH7 at an E:T ratio of 4:1 for 24 h, as measured by ELISA. Un-transduced PD-1$^+$-T cells were used as controls (one-way ANOVA). Data are presented as the mean ± SD. *P<0.05 and ***P<0.001. ns, not significant; CAR, chimeric antigen receptor; PD-1, programmed death 1; GPC3, glypican-3; IFN, interferon; E:T, effector-to-target; FC, flow cytometry.

on double-target CAR-T cells, using un-infected T cells as controls.

Although there was no difference in PD-1 expression between the two classes of CAR-T cells, less lymphocyte activation gene 3 and T cell immunoglobulin and mucin-domain containing-3 were expressed in double-target CAR-T cells than in GPC3-CAR-T cells (Fig. 5A), confirming that PD-1 blockade prevents CAR-T cells from entering an exhausted state. CAR-T cell apoptosis during stimulation was then measured. When PD-1 was blocked, less double-target CAR-T cells were subjected to apoptosis (25.41% on day 24) (Fig. 5B), confirming the pro-survival effect of blocking PD-1 on CAR-T cells.

As revealed by RT-qPCR, double-target CAR-T cells expressed more Bcl-2 (anti-apoptotic; Fig. 5C) and less caspase-3 (pro-apoptotic; Fig. 5D) compared with GPC3-CAR-T cells, which is indicative of the resistance of double-target CAR-T cells to apoptosis. Double-target CAR-T cells also exhibited enhanced long-term proliferation capacity throughout the extended culture, as compared with GPC3-CAR-T cells (Fig. 5E). Beyond that, as the provoking increased, a higher proportion of double-target CAR-T cells presented stem-like-memory (CD62L$^+$CD45RA$^+$) phenotype (17.68% on Day 24) than that of GPC3-CAR-T cells (7.37% on day 24; Fig. 5F).

In conclusion, the blocking of PD-1 provides CAR-T cell exhaustion resistance, antiapoptotic, and low terminal differentiation properties in long-term antigen stimulation.

Double-target CAR-T cells have superior anti-tumor effects in the TX model mice. The tumour-resistant property of double-target CAR-T cells was assessed *in vivo* by modeling HuH7 tumour-bearing NOD/SCID mice. As detailed in Fig. 6A, each mouse received an intra-tumoral injection of 10^6 CAR-T cells. In the group composed of CAR-T cells combined with anti-PD-1 antibody, 150 mg mAbs against PD-1 were intraperitoneally injected into each mouse for 5 weeks (once a week). It was revealed that tumors in mice undergoing double-target CAR-T cell treatment grew slower than those in mice receiving combined regimen and GPC3-CAR-T cells (Fig. 6B and C). In addition, a more notable survival benefit was observed in double-target CAR-T cells compared with GPC3-CAR-T cells (Fig. 6D).

IHC was then performed to measure Ki-67, VEGF-A and MMP-9 expression in the tumour tissues. Tumor tissue treated with the dual-function CAR-T cells expressed lower levels of

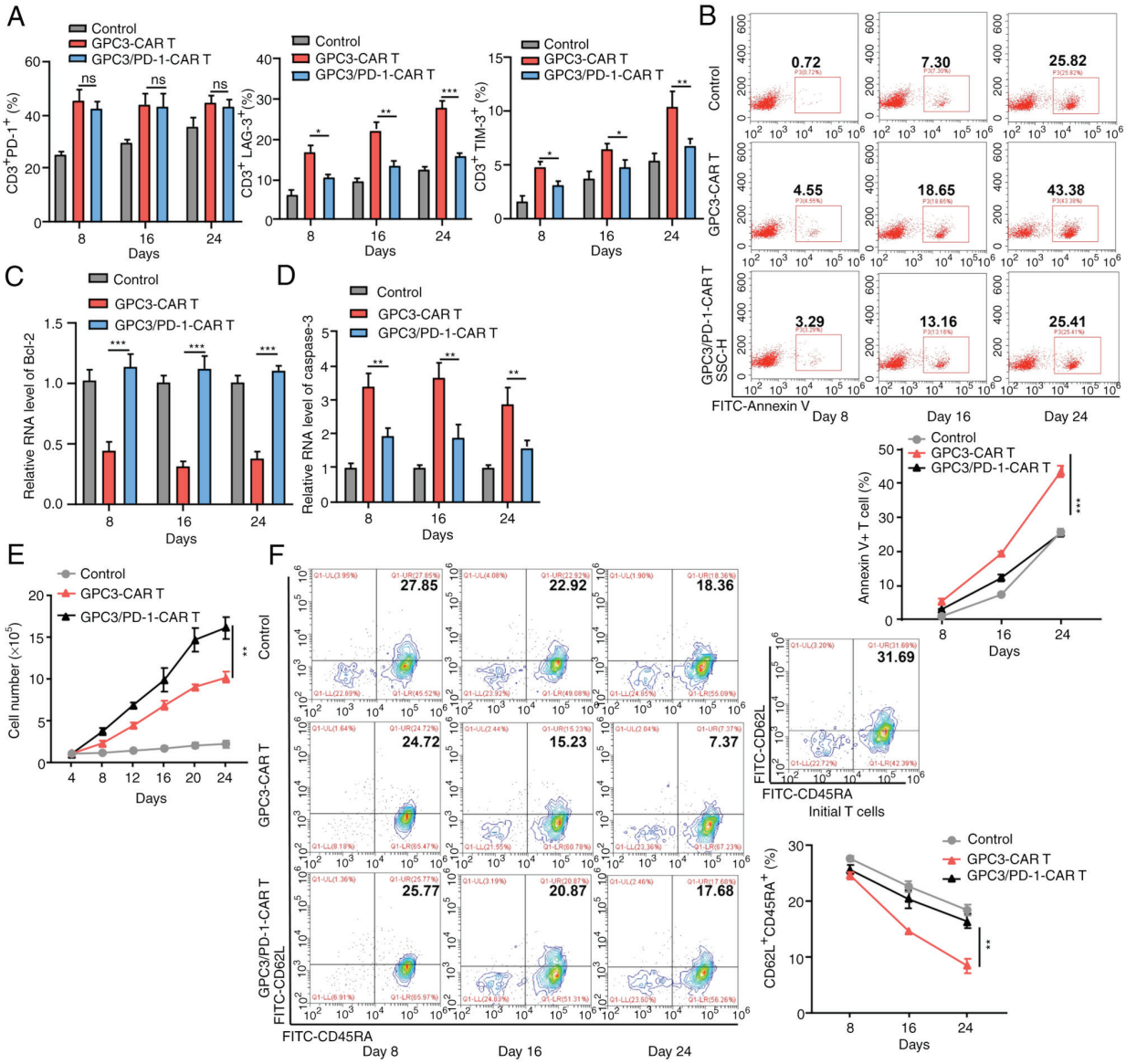

Figure 5. Double-target CAR-T cells display downgraded IR expression, strengthened proliferation capability, and subdued terminal differentiation in long time antigen provoking. (A) Expression levels of PD-1, LAG-3 and TIM-3 in each group at 8, 16 and 24 days in the long-run provoking process. (B) Annexin V+ cell percentage in each group at 8, 16 and 24 days in the long-run provoking process. (C and D) Levels of Bcl-2 and caspase-3 in CAR-T cells on days 8, 16 and 24 in the long-run provoking process examined using reverse transcription-quantitative PCR. (E) Alterations in the total cell number in each group during long-run provoking every 4 days (two-way ANOVA). (F) The expression of CD62L and CD45RA on the CAR-T cells and initial T cells in each group in the long-run provoking process. Data are presented as the mean ± SD. *P<0.05, **P<0.01 and ***P<0.001. ns, not significant. CAR, chimeric antigen receptor; IR, inhibitory receptor; PD-1, programmed death 1; LAG-3, lymphocyte-activation gene 3; TIM-3, T cell immunoglobulin and mucin-domain containing-3.

Ki-67, VEGF-A and MMP-9, indicating that the dual-function CAR-T cells have greater activation in suppressing the proliferation, angiogenesis and metastasis of the tumor cells (Fig. 6E). Furthermore, the group treated with dual-function CAR-T cells exhibited a higher frequency of total T cells within tumor tissue (Fig. 6F).

Discussion

Anti PD-1/PD-L1 monoclonal antibodies have been used in clinical research and the results are very promising. In particular, atezolizumab (anti-PD-L1 mAb), nivolumab (anti-PD1 mAb), and pembrolizumab (anti-PD1 mAb) have already been approved with durable clinical response and prolonged overall survival, reaching clinics for the treatment of melanoma, non-small cell lung cancer, and renal cell carcinoma (24,25). However, this treatment is greatly limited by its low response rates in certain types of cancer, lack of known biomarkers, immune-related toxicity, innate and acquired drug resistance (26). Precisely speaking, the response rate of most cancers is not greater than 30%, which results in a limited therapeutic efficacy (27). As a new type of immunotherapy, CAR-T has attracted much attention due to its specific killing of tumor cells. Jiang *et al* (28) established a bispecific CAR targeting tyrosine-protein kinase Met and PD-L1 and proved that these bispecific CAR-T cells have enhanced therapeutic effects on HCC. Yuan *et al* (29) established a bispecific CAR targeting c-Met and PD-1 and proved that these bispecific CAR-T cells exhibited potent anti-tumor efficacy in solid tumors. In the present study, a new-class double-target CAR

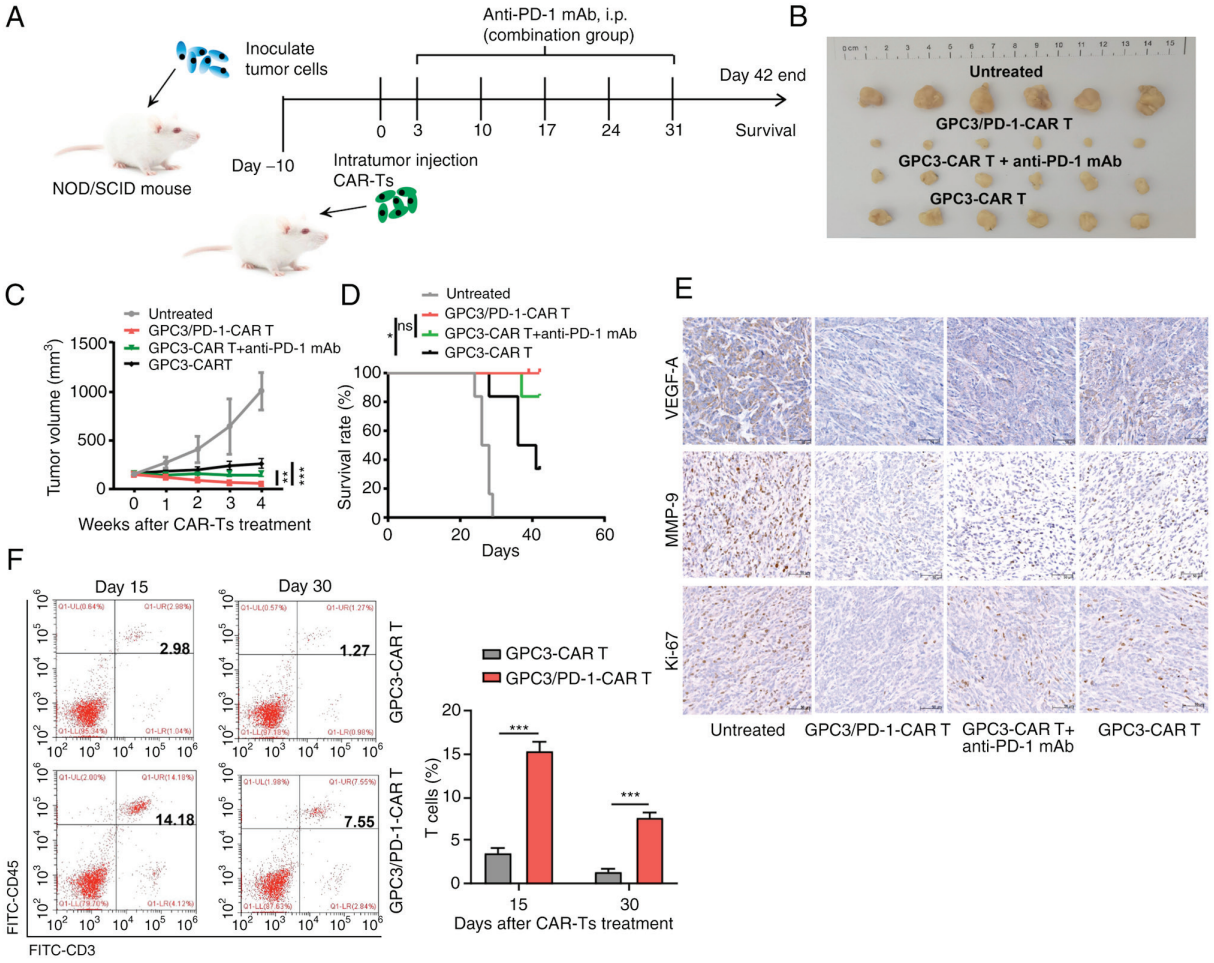

Figure 6. Dual-function CAR-T cells have superior anti-tumor effect in xenograft models of HuH7 tumour cells. (A) Diagram of the treatment strategy. (B) Xenograft tumours. (C) Changes in the mean tumour volume following CAR-T cell treatment. (D) Kaplan-Meier survival curves of different groups. (E) Characteristic images of Ki-67, VEGF-A and MMP-9 expression levels in each group of tumour tissues, as evaluated by immunohistochemistry (magnification, x20). (F) Proportion of tumour-infiltrating T cells in each group at 15 and 30 days after treatment (left). Data are presented as the mean ± SD. **P<0.01 and ***P<0.001. ns, not significant; CAR, chimeric antigen receptor; TX, tumour xenograft; VEGF, vascular endothelial growth factor.

that recognizes GPC3 and blocks PD-1 was established. Compared with c-Met, GPC3 is more specifically upregulated in HCC (30,31). Blocked PD-1 markedly increased the toxicity of CAR-T cells *in vitro*. On the other hand, *in vivo* assays revealed the hindering effect of double-target CAR-T cells on tumour growth and their promoting effect in extending the survival of tumour-bearing mice, as compared with their single-target counterparts. Beyond that, double-target CAR-T cells exhibited enhanced persistence, limited inhibitory receptor expression, and less differentiated phenotypes in tumour tissues, giving rise to more potent tumour-resisting effects than their single-target counterparts.

CAR-T therapy has achieved effective responses in relapsed B-cell leukemia and lymphoma (32-34). However, there are still many difficulties in the application of CAR-T in the therapy of solid tumors (35-37). Following in-depth research, the PD-1/PD-L1 pathway has been accepted as a pivotal hallmark in checkpoint blockade treatment (38,39). It has been shown by pre-clinical studies that PD-1/PD-L1 mAbs combined with CAR-T cells can jointly suppress tumours (40-42). Impacted by PD-1 blocking, the newly established double-target CAR-T cells displayed resistance to the suppression of the PD-1/PD-L1 pathway, and their toxicity remained unchanged in PD-L1$^+$ tumors. On the other hand, secreting perforin and GrB is one of primary ways of CAR-T cell toxicity (43,44). It was evidenced herein that, in contrast to tumour cells, T cells were more tolerant to GrB and perforin, providing one explanation for the targeting effect of double-target CAR-T cells on PD-1$^+$ tumour cells.

The limitations of the TX model are evident. The findings of *in-vivo* experiments were principally based on the interplay between CAR-T and tumour cells. However, certain immune cells in the TME, such as endogenous tumour-infiltrating T cells, myeloid-derived suppressor cells and dendritic cells, also express PD-L1, exerting markedly affecting tumour outcome. In addition, nude mice deficient in normal immune function were selected as research objects; other breeds will be used for future modelling. In addition, the lack of comparison between CAR-T cell therapy and PD-1/PD-L1 antibodies is a limitation to the present study. Furtermore, the lack of CAR-T cell proliferation detection is another limitation.

In conclusion, impacted by PD-1 blocking, the newly constructed double-target CAR-T cells exhibit stronger tumour-suppressing effects on HCC than common single-target CAR-T cells. The present study provided new ideas for the successful treatment of solid tumors by CAR-T cell therapy.

Acknowledgements

Not applicable.

Funding

The present study was supported by the Sanming Project of Medicine in Shenzhen (grant no. SZSM201612071), the Shenzhen Key Medical Discipline Construction Fund (grant no. SZXK078) and the The Cell Technology Center and Transformation Base, Innovation Center of Guangdong-Hong Kong-Macao Greater Bay Area, Ministry of Science and Technology of China [grant no. YCZYPT (2018)03-1].

Availability of data and materials

The datasets used and/or analyzed during the current study are available from the corresponding author on reasonable request.

Authors' contributions

JC and WVZ conceived the study. TZ, YL and XC curated the data. TZ, YL and ZC reanalyzed the data. DL and JQ were responsible for the study methodology. DL was responsible for the resources. JC and WVZ supervised the study. All authors wrote, reviewed and edited the original draft. All authors read and approved the final manuscript. JC and WVZ confirm the authenticity of all the raw data.

Ethics approval and consent to participate

All experimental procedures in the present study were approved (approval no. 2021-081) by the Ethics Committee of Peking University Shenzhen Hospital (Shenzhen, China). Written informed consent was obtained from all human peripheral blood donors.

Patient consent for publication

Not applicable.

Competing interests

The authors declare that they have no competing interests.

References

1. Yin H, Sun L, Pu Y, Yu J, Feng W, Dong C, Zhou B, Du D, Zhang Y, Chen Y and Xu H: Ultrasound-Controlled CRISPR/Cas9 system augments sonodynamic therapy of hepatocellular carcinoma. ACS Cent Sci 7: 2049-2062, 2021.
2. Sung H, Ferlay J, Siegel RL, Laversanne M, Soerjomataram I, Jemal A and Bray F: Global cancer statistics 2020: GLOBOCAN estimates of incidence and mortality worldwide for 36 cancers in 185 countries. CA Cancer J Clin 71: 209-249, 2021.
3. Lai JP, Sandhu DS, Yu C, Han T, Moser CD, Jackson KK, Guerrero RB, Aderca I, Isomoto H, Garrity-Park MM, *et al*: Sulfatase 2 up-regulates glypican 3, promotes fibroblast growth factor signaling, and decreases survival in hepatocellular carcinoma. Hepatology 47: 1211-1222, 2008.
4. Cabibbo G, Enea M, Attanasio M, Bruix J, Craxi A and Camma C: A meta-analysis of survival rates of untreated patients in randomized clinical trials of hepatocellular carcinoma. Hepatology 51: 1274-1283, 2010.
5. Wei Y, Tang X, Ren Y, Yang Y, Song F, Fu J, Liu S, Yu M, Chen J, Wang S, *et al*: An RNA-RNA crosstalk network involving HMGB1 and RICTOR facilitates hepatocellular carcinoma tumorigenesis by promoting glutamine metabolism and impedes immunotherapy by PD-L1+ exosomes activity. Signal Transduct Target Ther 6: 421, 2021.
6. Gao W, Kim H, Feng M, Phung Y, Xavier CP, Rubin JS and Ho M: Inactivation of Wnt signaling by a human antibody that recognizes the heparan sulfate chains of glypican-3 for liver cancer therapy. Hepatology 60: 576-587, 2014.
7. Knelson EH, Gaviglio AL, Nee JC, Starr MD, Nixon AB, Marcus SG and Blobe GC: Stromal heparan sulfate differentiates neuroblasts to suppress neuroblastoma growth. J Clin Invest 124: 3016-3031, 2014.
8. Cui X, Li Z, Gao PJ, Gao J and Zhu JY: Prognostic value of glypican-3 in patients with HBV-associated hepatocellular carcinoma after liver transplantation. Hepatobiliary Pancreat Dis Int 14: 157-163, 2015.
9. Fu SJ, Qi CY, Xiao WK, Li SQ, Peng BG and Liang LJ: Glypican-3 is a potential prognostic biomarker for hepatocellular carcinoma after curative resection. Surgery 154: 536-544, 2013.
10. Zhang Q, Han Z, Tao J, Zhao M, Zhang W, Li P, Tang L and Gu Y: An innovative peptide with high affinity to GPC3 for hepatocellular carcinoma diagnosis. Biomater Sci 7: 159-167, 2018.
11. Xia L, Teng Q, Chen Q and Zhang F: Preparation and characterization of anti-GPC3 nanobody against hepatocellular carcinoma. Int J Nanomedicine 15: 2197-2205, 2020.
12. Du K, Li Y, Liu J, Chen W, Wei Z, Luo Y, Liu H, Qi Y, Wang F and Sui J: A bispecific antibody targeting GPC3 and CD47 induced enhanced antitumor efficacy against dual antigen-expressing HCC. Mol Ther 29: 1572-1584, 2021.
13. Yu M, Luo H, Fan M, Wu X, Shi B, Di S, Liu Y, Pan Z, Jiang H and Li Z: Development of GPC3-specific chimeric antigen receptor-engineered natural killer cells for the treatment of hepatocellular carcinoma. Mol Ther 26: 366-378, 2018.
14. Shi D, Shi Y, Kaseb AO, Qi X, Zhang Y, Chi J, Lu Q, Gao H, Jiang H, Wang H, *et al*: Chimeric antigen receptor-glypican-3 T-cell therapy for advanced hepatocellular carcinoma: Results of phase I trials. Clin Cancer Res 26: 3979-3989, 2020.
15. Kang CH, Kim Y, Lee DY, Choi SU, Lee HK and Park CH: c-Met-Specific chimeric antigen receptor T cells demonstrate anti-tumor effect in c-met positive gastric cancer. Cancers (Basel) 13: 5738, 2021.
16. Mansilla-Soto J, Eyquem J, Haubner S, Hamieh M, Feucht J, Paillon N, Zucchetti AE, Li Z, Sjostrand M, Lindenbergh PL, *et al*: HLA-independent T cell receptors for targeting tumors with low antigen density. Nat Med 28: 345-352, 2022.
17. Wang SS, Luong K, Gracey FM, Jabar S, McColl B, Cross RS and Jenkins MR: A novel peptide-MHC targeted chimeric antigen receptor T cell forms a T cell-like immune synapse. Biomedicines 9: 1875, 2021.
18. Tsimberidou AM, Van Morris K, Vo HH, Eck S, Lin YF, Rivas JM and Andersson BS: T-cell receptor-based therapy: An innovative therapeutic approach for solid tumors. J Hematol Oncol 14: 102, 2021.
19. Consonni M, Garavaglia C, Grilli A, de Lalla C, Mancino A, Mori L, De Libero G, Montagna D, Casucci M, Serafini M, *et al*: Human T cells engineered with a leukemia lipid-specific TCR enables donor-unrestricted recognition of CD1c-expressing leukemia. Nat Commun 12: 4844, 2021.
20. Hu J, Yang Q, Zhang W, Du H, Chen Y, Zhao Q, Dao L, Xia X, Natalie Wall F, Zhang Z, *et al*: Cell membrane-anchored and tumor-targeted IL-12 (attIL12)-T cell therapy for eliminating large and heterogeneous solid tumors. J Immunother Cancer 10:e003633, 2022.
21. Meyran D, Terry RL, Zhu JJ, Haber M, Ziegler DS, Ekert PG, Trapani JA, Darcy PK and Neeson PJ: Early-phenotype CAR-T cells for the treatment of pediatric cancers. Ann Oncol 32: 1366-1380, 2021.
22. Lemoine J, Ruella M and Houot R: Born to survive: How cancer cells resist CAR T cell therapy. J Hematol Oncol 14: 199, 2021.
23. Greenbaum U, Dumbrava EI, Biter AB, Haymaker CL and Hong DS: Engineered T-cell receptor T cells for cancer immunotherapy. Cancer Immunol Res 9: 1252-1261, 2021.
24. Livak KJ and Schmittgen TD: Analysis of relative gene expression data using real-time quantitative PCR and the 2(-Delta Delta C(T)) method. Methods 25: 402-408, 2001.
25. Sharma P and Allison JP: Immune checkpoint targeting in cancer therapy: Toward combination strategies with curative potential. Cell 161: 205-214, 2015.

26. Wu M, Huang Q, Xie Y, Wu X, Ma H, Zhang Y and Xia Y: Improvement of the anticancer efficacy of PD-1/PD-L1 blockade via combination therapy and PD-L1 regulation. J Hematol Oncol 15: 24, 2022.
27. Shen N, Yang C, Zhang X, Tang Z and Chen X: Cisplatin nanoparticles possess stronger anti-tumor synergy with PD1/PD-L1 inhibitors than the parental drug. Acta Biomater 135: 543-555, 2021.
28. Jiang W, Li T, Guo J, Wang J, Jia L, Shi X, Yang T, Jiao R, Wei X, Feng Z, *et al*: Bispecific c-Met/PD-L1 CAR-T cells have enhanced therapeutic effects on hepatocellular carcinoma. Front Oncol 11: 546586, 2021.
29. Yuan X, Sun Z, Yuan Q, Hou W, Liang Q, Wang Y, Mo W, Wang H and Yu M: Dual-function chimeric antigen receptor T cells targeting c-Met and PD-1 exhibit potent anti-tumor efficacy in solid tumors. Invest New Drugs 39: 34-51, 2021.
30. Zheng X, Liu X, Lei Y, Wang G and Liu M: Glypican-3: A novel and promising target for the treatment of hepatocellular carcinoma. Front Oncol 12: 824208, 2022.
31. Sun L, Gao F, Gao Z, Ao L, Li N, Ma S, Jia M, Li N, Lu P, Sun B, *et al*: Shed antigen-induced blocking effect on CAR-T cells targeting Glypican-3 in hepatocellular carcinoma. J Immunother Cancer 9: e001875, 2021.
32. Jacoby E, Shahani SA and Shah NN: Updates on CAR T-cell therapy in B-cell malignancies. Immunol Rev 290: 39-59, 2019.
33. Gauthier J, Bezerra ED, Hirayama AV, Fiorenza S, Sheih A, Chou CK, Kimble EL, Pender BS, Hawkins RM, Vakil A, *et al*: Factors associated with outcomes after a second CD19-targeted CAR T-cell infusion for refractory B-cell malignancies. Blood 137: 323-335, 2021.
34. Frigault MJ, Dietrich J, Martinez-Lage M, Leick M, Choi BD, DeFilipp Z, Chen YB, Abramson J, Crombie J, Armand P, *et al*: Tisagenlecleucel CAR T-cell therapy in secondary CNS lymphoma. Blood 134: 860-866, 2019.
35. Zhang ZZ, Wang T, Wang XF, Zhang YQ, Song SX and Ma CQ: Improving the ability of CAR-T cells to hit solid tumors: Challenges and strategies. Pharmacol Res 175: 106036, 2022.
36. Shen L, Xiao Y, Tian J and Lu Z: Remodeling metabolic fitness: Strategies for improving the efficacy of chimeric antigen receptor T cell therapy. Cancer Lett 529: 139-152, 2022.
37. Dana H, Chalbatani GM, Jalali SA, Mirzaei HR, Grupp SA, Suarez ER, Raposo C and Webster TJ: CAR-T cells: Early successes in blood cancer and challenges in solid tumors. Acta Pharm Sin B 11: 1129-1147, 2021.
38. Akbari P, Huijbers EJM, Themeli M, Griffioen AW and van Beijnum JR: The tumor vasculature an attractive CAR T cell target in solid tumors. Angiogenesis 22: 473-475, 2019.
39. Dammeijer F, van Gulijk M, Mulder EE, Lukkes M, Klaase L, van den Bosch T, van Nimwegen M, Lau SP, Latupeirissa K, Schetters S, *et al*: The PD-1/PD-L1-checkpoint restrains T cell immunity in tumor-draining lymph nodes. Cancer Cell 38: 685-700.e8, 2020.
40. Wang Z, Li N, Feng K, Chen M, Zhang Y, Liu Y, Yang Q, Nie J, Tang N, Zhang X, *et al*: Phase I study of CAR-T cells with PD-1 and TCR disruption in mesothelin-positive solid tumors. Cell Mol Immunol 18: 2188-2198, 2021.
41. Kato D, Yaguchi T, Iwata T, Katoh Y, Morii K, Tsubota K, Takise Y, Tamiya M, Kamada H, Akiba H, *et al*: GPC1 specific CAR-T cells eradicate established solid tumor without adverse effects and synergize with anti-PD-1 Ab. Elife 9: e49392, 2020.
42. Shi X, Zhang D, Li F, Zhang Z, Wang S, Xuan Y, Ping Y and Zhang Y: Targeting glycosylation of PD-1 to enhance CAR-T cell cytotoxicity. J Hematol Oncol 12: 127, 2019.
43. Restifo NP, Dudley ME and Rosenberg SA: Adoptive immunotherapy for cancer: harnessing the T cell response. Nat Rev Immunol 12: 269-281, 2012.
44. O'Connell J, O'Sullivan GC, Collins JK and Shanahan F: The Fas counterattack: Fas-mediated T cell killing by colon cancer cells expressing Fas ligand. J Exp Med 184: 1075-1082, 1996.